Reliability and Reproducibility of the Cryogenic Sapphire Oscillator Technology

Christophe Fluhr[▽], Benoît Dubois[▽], Guillaume Le Tetu[♯], Valerie Soumann[♯], Julien Paris[♭], Enrico Rubiola[♯⊗] and Vincent Giordano[♯◇]

***Abstract*—The cryogenic sapphire oscillator (CSO) is a highly specialized machine, which delivers a microwave reference signal exhibiting the lowest frequency fluctuations (Allan deviation $\sigma_y(\tau)$) for the integration time τ between 1 s and 10^4 s, indeed 4 decades. In such interval, good units feature $\sigma_y(\tau) < 10^{-15}$, with $< 10^{-14}$ drift in one day. The oscillator is based on a sapphire monocrystal resonating at 10 GHz in a whispering-gallery mode, cooled at $\approx$ 6 K for zero thermal coefficient and optimal quality factor Q. We report on the progress accomplished implementing eleven CSOs in about 10 years since the first sample delivered to the Malargüe station of the European Space Agency (ESA) in Argentina. Short-term stability is improved by a factor of 3–10, depending on τ, and the refrigerator's electric power is reduced to 3 kW single-phase line. Frequency stability and overall performances are reproducible, with unattended operation between scheduled maintenance every two years. The CSO is now a semicommercial product suitable to scientific applications requiring extreme frequency stability with reliable unattended long-term operation, like the flywheel for primary frequency standards, the ground segment of Global Navigation Satellite System (GNSS), astrometry, Very Long Baseline Interferometry, and radio astronomy stations.**

***Index Terms*—Time and frequency metrology, Ultra-stable oscillators, Cryogenic oscillators, Sapphire resonator, Frequency stability.**

I. Introduction

AFTER pioneering work on the superconducting cavity [1], [2], it was the cryogenic sapphire-loaded cavity that caught the researchers' attention. Significant work was carried on mainly at Jet Propulsion Laboratory (JPL)[3], at University of Western Australia (UWA)[4], at National Physical Laboratory (NPL)[5] and at the Laboratoire de Physique et Métrologie des Oscillateurs[6] (now Institut FEMTO-ST). In the late 1990s, Cryogenic Sapphire Oscillators (CSOs) demonstrated short-term fractional frequency stability of the order of 10^{-15} Allan deviation $\sigma_y(\tau)$ with the resonator in liquid-He bath [7], [8]. Then, breakthrough performances and early uses in Time and Frequency Metrology have been demonstrated in the early 2000s, still with He bath [9], [10], [11], [12], [13]. The JPL pioneered the implementation with pulse-tube cryocoolers [14] and we followed, keeping the frequency stability at the state of the art [15].

Eventually, NPL and JPL lost interest in the field, and the Australian research moved to the University of Adelaide starting a business under the brand Quantx (formerly Cryoclock) [16].

On the French side, we focused on engineering. We improved the immunity to environmental perturbations [17], [18], we rationalized the design, and we improved the long-term stability [19]. However, the toughest challenge was to reduce the power needed by the refrigerator from 380 V, 6–8 kW three-phase of the first prototypes to 3 kW single-phase [20], so that the CSO can be powered by a regular outlet (230 V 50 Hz, or 117 V, 60 Hz). Our CSOs evolved into a semicommercial product code named ULISS-2G, available from FEMTO-Engineering (a no-profit company owned by uFC, a Gov university) to qualified users. Describing the (in)stability as the Allan deviation (ADEV) $\sigma_y(\tau)$ of the fractional frequency y as a function of the measurement time τ, ULISS-2G features $\sigma_y(\tau) < 3{\times}10^{-15}$ at $\tau = 1$ s, decreasing to parts in 10^{-16} at longer τ, and limited by a drift of 10^{-14} max at one day. It can run unattended for years of continuous operation, with only simple maintenance every 2nd year. .

The integration time $1\text{ s} < \tau < 10^4$ s is a challenging region, where there is no competing technology. The Hydrogen maser and the laser stabilized to a Fabry-Pérot cavity are the closest options, but they are not a valid replacement for the CSO. The maser is a mature commercial product requiring 0.5 m^2 footprint, which may run unattended for 10 years on 100–200 W electric power. However, its short-term instability is significantly higher than the CSO, starting from $\sigma_y(\tau) \approx 10^{-13}$ at $\tau = 1$ s, decreasing at longer τ, and equating the CSO at τ of the order of one hour. The laser stabilized to a cryogenic Fabry-Pérot cavity may outperform the CSO at short τ [21], [22], yet with similar or higher drift. However, the main problem is that such machines are laboratory experiments, with no commercial option available. The resonator, a Fabry-Pérot étalon, is a bulky piece of semiconductor-grade Silicon, typically 10–20 cm long, placed in a liquid-He refrigerator which is likely larger than ours. Additionally, a metrological femtosecond comb is required to deliver an RF or microwave signal locked to the laser. The unattended operation is limited by occasional random unlocking of the laser or of the comb. Commercial lasers stabilized on a room temperature Ultra-

Manuscript submitted September 2022, revised February 2023. This work is partially funded by the Agence Nationale de Recherche (ANR) Programme d'Investissement d'Avenir under the following grants: ANR-11-EQPX-0033-OSC-IMP (Oscillator IMP project) ANR-10-LABX-48-01 (FIRST-TF network), and ANR-17-EURE-00002 (EIPHI); by the French RENATECH network and its FEMTO-ST technological facility, and by grants from the Région Bourgogne Franche Comté intended to support the above.

▽ FEMTO-Engineering, 25000 Besançon, France.

♯ Institut FEMTO-ST, Centre National de la Recherche Scientifique (CNRS), Université de Franche Comté (uFC), SUPMICROTECH-ENSMM, 25000 Besançon, France.

♭ MyCryoFirm, 94120 Fontenay-sous-Bois, France.

⊗ Istituto Nazionale di Ricerca Metrologica INRiM, Torino, Italy.

◇ *Corresponding author Vincent Giordano,* e-mail giordano@femto-st.fr

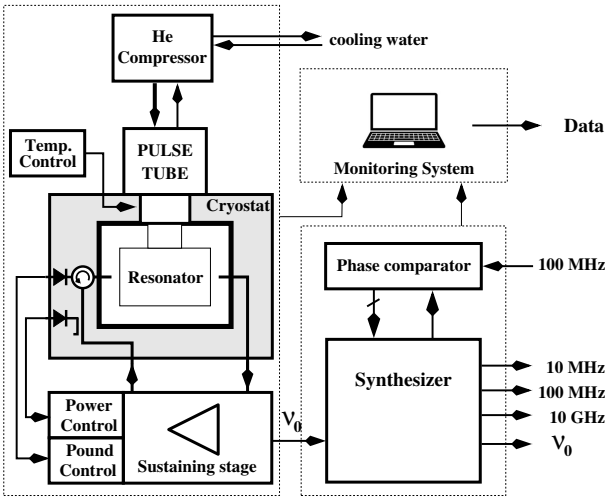

Figure 1. CSO block diagram: we distinguish 3 mains subsets: the ultra-stable oscillator itself, the frequency synthesizer and the monitoring system.

Low Expansion (ULE) Fabry-Pérot étalon approach the short-term stability of the CSO at short τ, but the drift is still $10^{-11} \ldots 10^{-12}$/day [23], [24], and the femtosecond comb is necessary to get a RF signal.

The CSO shines in applications where extremely low instability $\sigma_y(\tau)$ is critical, for measurement time τ up to 10^4 s, and reliable unattended long-term operation is required. This is the case of the flywheel for primary frequency standards, and of the ground segment of Global Navigation Satellite System (GNSS). Other applications are found in astrometry, in Very Long Baseline Interferometry (VLBI), and in radio astronomy stations. Best stability at $1\text{ s} < \tau < 10^4$ s means that the CSO is a great candidate for the exploration of the solar system. For reference, light travels the Moon's semi-major axis in 1.3 s, one Astronomical Unit AU (or the semi-major axis of the Earth orbit) in 499 s, and the Jupiter's and Uranus' semi-major axis in 2595 and 9576 s, respectively.

After a review of the key points of the technology and the historical development, we provide unique information about the reproducibility and reliability gathered in 15 years of experience, namely (i) the spread of resonant frequency, turnover temperature and quality factor of 17 resonators from 3 manufacturers, tested at liquid-He temperature, (ii) the Allan deviation $\sigma_y(\tau)$ of 11 CSOs, for τ from 1 s to 1 day, and (iii) anecdotal facts about transporting such CSOs, with or without disassembling.

II. FEMTO-ST CSO Design

Fig. 1 shows the block diagram of the CSO. The high Q sapphire resonator is maintained near 6 K in a cryostat cooled by an autonomous Pulse-Tube (PT) cryocooler. The CSO is a Pound-Galani oscillator, where the resonator is used in transmission mode in a regular oscillator loop, and in reflection mode as the discriminator of the classical Pound servo. The sustaining stage and the control electronics are at room temperature. The CSO output signal at the resonator frequency ν_0 drives the synthesizer, which delivers 10 GHz, 100 MHz and 10 MHz output frequencies in a typical implementation.

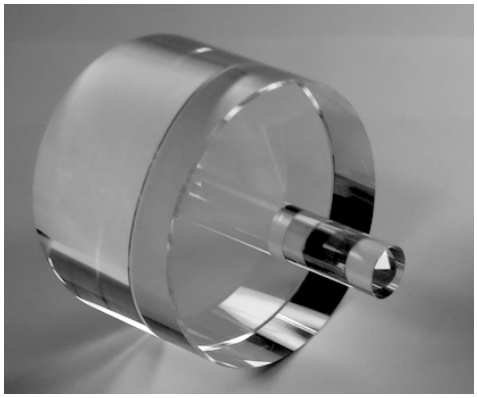

Figure 2. Sapphire resonator at 9.99 GHz in $\text{WGH}_{15,0,0}$ mode.

The synthesizer outputs can be disciplined at long term on an external 100 MHz signal, for example from a Hydrogen Maser. A computer records continuously the parameters relevant to the CSO status. The technological choices relating to the various subsets have already been described in previous publications to which we refer the reader [25], [26], [27], [28]. Here, we recall the key features making the originality of our design.

A. Sapphire Resonator

The resonator (Fig. 2) is a cylinder of sapphire monocrystal of 54 mm diameter and 30 mm high, resonating in quasi-transverse magnetic whispering-gallery mode $\text{WGH}_{15,0,0}$ at $\nu_0 = 9.99\text{ GHz} \pm 5\text{ MHz}$. This choice greatly simplifies the design of the frequency synthesis (see below). The resonant frequency shows a turnover temperature T_0 near 6 K, where the resonator sensitivity to temperature nulls at first order. Such turning point results from paramagnetic impurities of Cr^{3+} or Mo^{3+} in the Al_2O_3 lattice, whose typical mass concentration is well below 1 ppm. The exact value of T_0 is a specific parameter of each resonator, typically found between 5 K and 9 K in the high-quality crystals we use [29]. At T_0, the unloaded Q factor is up to two billions, depending on the crystal quality, on the resonator adjustment, and on cleaning. The spindle seen in Fig. 2 is machined from the bulk together with the resonator. This geometry ensures that the resonator can be mounted with no stress in the circumferential region, where the microwave energy is located.

The resonator is inserted in the center of a cylindrical cavity made of standard Oxygen-free high-thermal-conductivity (OFHC) Copper, electromagnetically coupled to 2.2-mm semi-rigid cables via two small loops. Optimal operation requires critical coupling at the resonator input, so that the reflection coefficient is $S_{11}(\nu_0) \approx 0$. The technical difficulty is that the resonator coupling is proportional to Q, which is multiplied by some 10,000 when the temperature is decreased from room to ≈ 6 K. We developed a specific procedure requiring only two cool-down iterations. Fig. 3 shows the reflection coefficient at the input port, close to optimal coupling. Near-critical coupling proved to be stable for years, and resistant to travels.

Since 2009, we have purchased more than 25 sapphire resonators from several manufacturers selected after preliminary

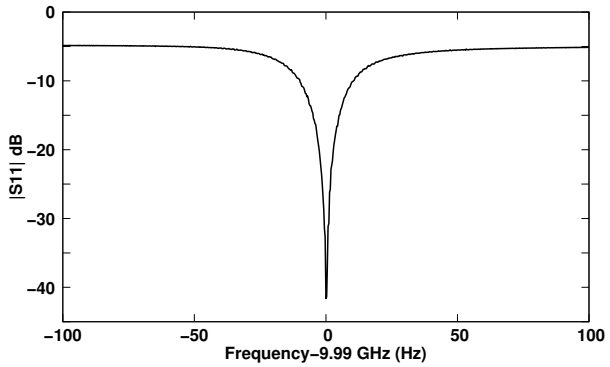

Figure 3. Reflection coefficient $|S_{1\,1}|$ of the $\mathrm{WGH}_{15,0,0}$ mode at liquid-He temperature.

tests on samples. Only 17 of such resonators were actually tested at liquid-He temperature. Fig. 4 shows the spread of the key values, ν_0, T_0 and unloaded Q of such resonators, and discussed below. The brands are labeled A: Crystal System, Llc. USA, B: Precision Sapphire Technologies, Ltd. Lithuania and C: Shinkosha Co., Ltd. Japan.

1) Resonant frequency ν_0: tight machining tolerances ensure that the resonant frequency is $\nu_0 = 9.99\ \mathrm{GHz} \pm 5\ \mathrm{MHz}$. This is intended to simplify the design of frequency synthesis (CF Sec. II-C). The resonators slightly out of specs are still usable without compromising the frequency stability, after minor modifications to the synthesis.

2) Turnover temperature T_0: the minimum value is of 4.6 K. A resonator having a lower turnover temperature cannot be used in the new ULISS-2G design, because the low-power refrigerator cannot safely cool it down with a sufficient margin for proper temperature stabilization. Oppositely, $T_0 > 8$ K results in degraded short-term stability, $\sigma_y > 3{\times}10^{-15}$ up to $\tau = 100$ s (Sec. IV).

3) Unloaded quality factor Q_0: The gain of the Pound frequency discriminator is proportional to loaded quality factor Q_L, which in our case is half of the unloaded quality factor Q_0. For the fractional frequency instability at the CSO output to be lower than $\sigma_y(\tau) = 1{\times}10^{-15}$ at $\tau = 1$ s, the minimum quality factor is $Q_0 = 5{\times}10^8$ [29]. All the resonators tested fulfil this requirement. Besides crystal quality, the presence of small particles stuck on the resonator surface limit the Q factor. We developed a cleaning method, done in a class 100 clean-room.

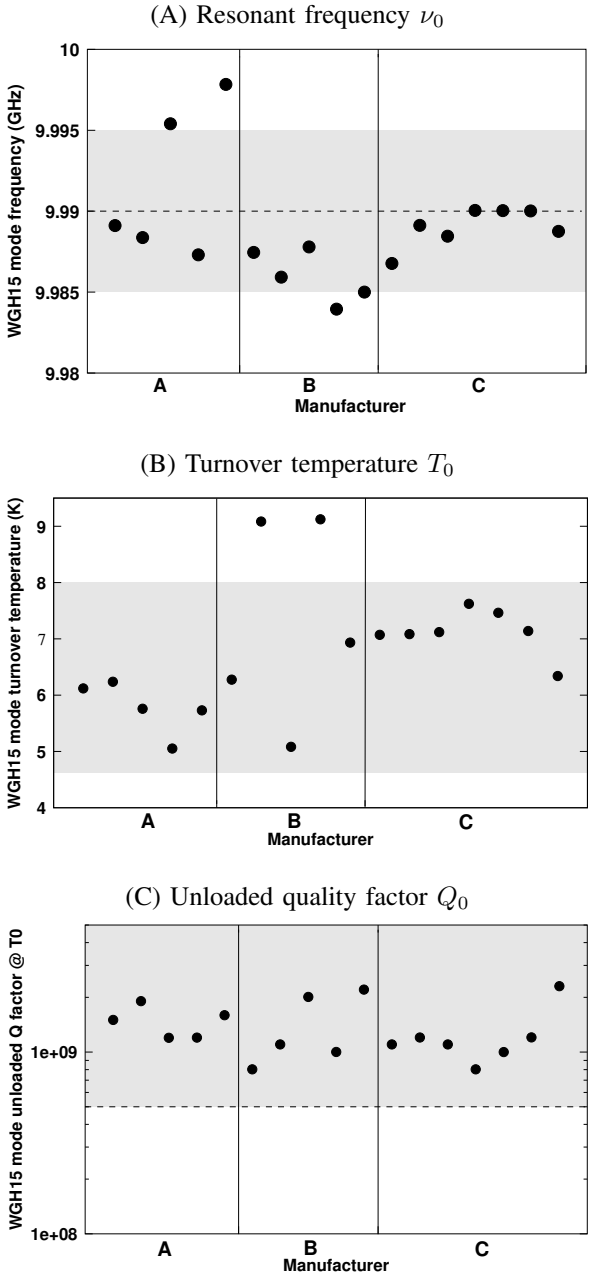

Figure 4. Parameters of the $\mathrm{WGH}_{15,0,0}$ mode for the resonators tested. Our specs are shown as the gray areas.

B. Sustaining Loop

The sustaining amplifier is at room temperature. It has 80 MHz bandwidth, determined by an internal bandpass filter centered on 9.99 GHz. Gain and phase lag are set independently by two external near-DC voltages, which are the actuator inputs for the power control and for the Pound frequency control. The phase modulation at the resonator input, necessary for the Pound control, has a frequency of 100 kHz. An internal coupler derives part of the loop signal to get the $10\ \mathrm{dBm} \pm 1\ \mathrm{dB}$ reference signal driving the frequency synthesizer.

The components in the cryostat near the resonator are the most critical. Microwave isolators and circulator are commercial SMA connectorized components that we selected after low temperature tests and cycling. The tunnel diodes for the power control and the Pound control [30] are electrically fragile because of the small band gap. To prevent degradation, we limit the power at the cryostat input to -5 dBm.

In some CSO designs [31], the frequency stability is affected by the residual amplitude modulation (RAM) in the Pound interrogation signal, which results in a frequency offset. This phenomenon is negligible in our case thanks to the low reflection coefficient at the resonator input. Thus, we do not implement a RAM-suppression control.

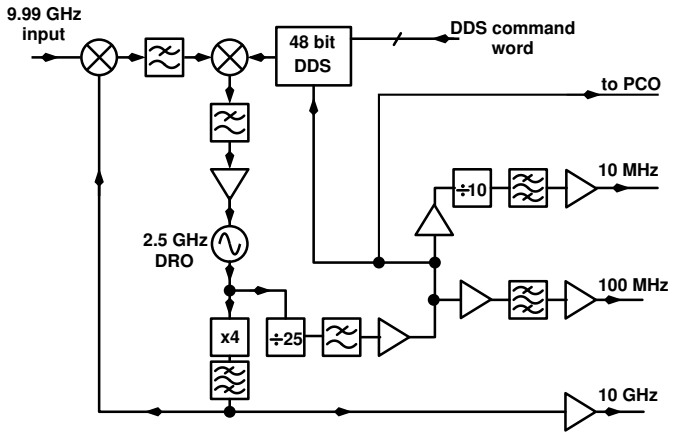

Figure 5. Synthesizer of the ULISS-2G CSO. VCO = Voltage Controlled Oscillator, DDS = Direct Digital Synthesizer, PCO = 100 MHz Phase COmparator.

C. Frequency Synthesis

The frequency synthesizer is shown in Fig. 5. A 2.5 GHz DRO selected for its low phase noise is frequency-multiplied to 10 GHz and phase-locked on the CSO output. The (10 ± 5) MHz gap between the 9.99 GHz sapphire output and multiplied DRO is compensated by adding the output of a low noise 48 bit DDS clocked at $\nu_{\rm ck} = 100$ MHz. The frequency resolution of the DDS is $\Delta\nu = \nu_{\rm ck}/2^{47} = 7.1{\times}10^{-7}$ Hz (only 47 bits of the 48 bit register contribute to the resolution). So, the fractional frequency resolution at the CSO output is $\Delta\nu/\nu_0 = 7.1{\times}10^{-17}$. The 100 MHz and 10 MHz output signals are generated by frequency division. The 100 MHz signal can also be send to the Phase Comparator (PCO) driven by an external reference signal. A digital control word is thus obtained to control the DDS frequency and discipline at long term the CSO synthesizer output signal.

D. Overview of 15 Years of Our Cryocooled CSOs

Since 2009, we built and validated eleven CSOs. Our first unit was build in the frame of the ELISA project, funded by the European Space Agency (ESA). In 2010, ELISA demonstrated for the first time a state-of-the-art frequency stability with an autonomous cryocooler, replacing the liquid helium bath [15]. As we will see in the next sections, our technology evolved in 2015 with the new design of a low-power cryocooler. Table I shows a summary of these CSOs.

III. ULISS-1G: 1ST GENERATION OF CRYCOOLED CSOS

The tradeoff in the cryostat design is to ensure a proper thermal conduction between the resonator and the cold source, while limiting the transfer of mechanical vibrations arising from the cryocooler. The ULISS-1G cryostat is shown in Fig. 6. We opted for simple solutions, favoring passive thermal filtering and mechanical decoupling by flexible links. The resonator is hold by stiff rods attached to a rigid frame, and thermally connected to the cold source by a set of copper braids. The fundamental frequency of the PT thermal cycle is typically ~ 1.4 Hz. The low-frequency vibration from the cold finger to the resonator is attenuated by the stiffness ratio of the copper braids to the holding rods. Moreover, the temperature variations on the cold finger are passively filtered by the thermal ballast constituted by the stainless steel top flange of the 2nd stage thermal shield. The thermal mass of the ballast and the thermal resistance of the braids are equivalent to a first order filter.

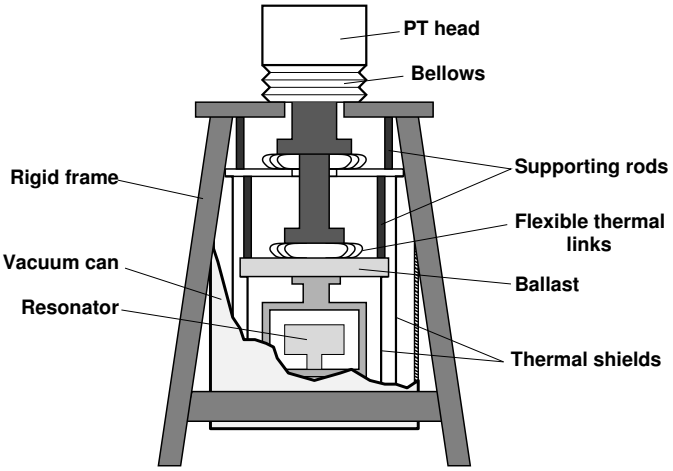

Figure 6. Cryostat of ULISS-1G.

For ULISS-1G we opted for a powerful cryocooler providing at least 500 mW cooling power at 4 K. Such a cooling power simplified the design and relaxed the constraints in the material and geometry of the holding rods and in the residual stiffness of the flexible thermal links. Thus, a temperature of 4 K and a residual displacement below 1 μm at the resonator level are easily reached.

ELISA was validated in 2010 in our lab, disassembled and packed, moved, and re-assembled at the ESA Deep Space Antenna Station DSA-3 in Malargüe, Argentina. More in detail, ELISA was transported by truck to Paris, by plane to Buenos Aires, and again by truck to destination, with the last 30 km on unpaved road. It did not suffer from vibrations and shocks. The resonator, the most fragile part, showed perfect coupling with no need for fine adjustment. Finally, ELISA was put into operation in only two days after arrival.

Encouraged by the success of ELISA, we decided to build three units for Oscillator IMP, our platform of metrology [32]. These 3 CSOs were implemented between 2010 and 2014, and progressively installed in a controlled environment, stabilized to $22\,^{\circ}\mathrm{C} \pm 0.5\,^{\circ}\mathrm{C}$ by a proportional-integral-derivative (PID) control. Since, they have been running almost continuously. Both, Pound and power servo loops, proved to be quite stable and robust, with no accidental loss of control ever detected. Several short stops were scheduled, for (i) routine replacing a filter in the Helium compressor every 2nd year, (ii) maintenance of the electrical installation in the building, and (iii) energy saving, during the first two weeks of August, when the lab is closed. We had only two failures, detailed in Section V.

Fig. 7 shows the fractional frequency stability of the ULISS-1G CSOs. The best unit features a short-term frequency stabil-

Table I
THE 11 CSOS BUILT AND VALIDATED AT THE FEMTO-ST INSTITUTE.

#	Nickname	Power	First operation	Status
000	ELISA	6 kW, 3-phase	June 2009	Prototype for ESA
001	MARMOTTE	6 kW, 3-phase	Oct. 2010	Oscillator IMP reference
002	ULISS	6 kW, 3-phase	Nov. 2011	Oscillator IMP reference, transportable unit
003	ABSOLUT	8 kW, 3-phase	May 2014	Oscillator IMP reference
004	ULISS-2G proto	3 kW, 1-phase	June 2015	Prototype, proof of principle
005	ULISS-2G 005	3 kW, 1-phase	Dec. 2017	Commercial, delivered
006	ULISS-2G 006	3 kW, 1-phase	Nov. 2018	Commercial, delivered
007	ULISS-2G 007	3 kW, 1-phase	June 2019	Commercial, delivered
008	ULISS-2G 008	3 kW, 1-phase	Dec. 2020	Commercial, delivered
009	ULISS-2G 009	3 kW, 1-phase	April 2021	Commercial, delivered
010	ULISS-2G 010	3 kW, 1-phase	March 2022	Commercial, validation in progress

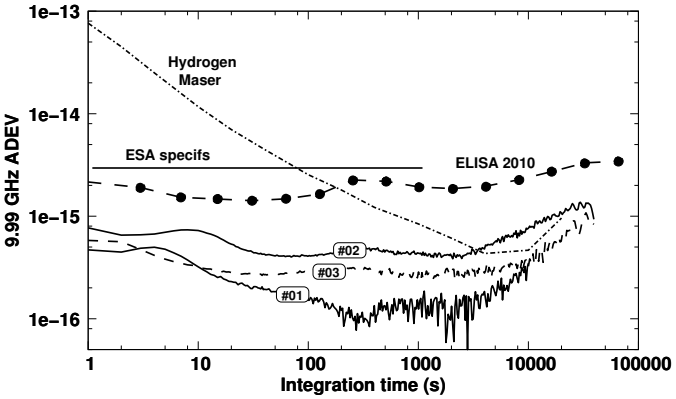

Figure 7. Fractional frequency stability of the ULISS-1G CSOs, after removing the linear drift, together with the specs of a high performances Hydrogen Maser. See Table I for the identification of the CSOs.

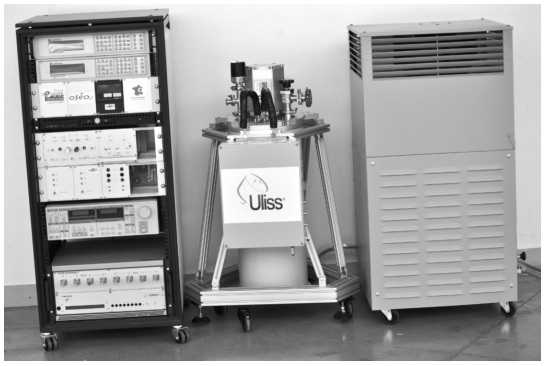

Figure 8. The CSO of 1st generation: ULISS-1G. Left: 19" rack including the electronic and temperature servos, the frequency synthesis; middle: the cryostat with the sustaining electronics (box in the front); right: air-cooled He compressor. This unit was designed to be transported in a small van to be tested in different sites around Europe. At home, the compressor is replaced with a water-cooled unit.

ity of $5\times10^{-16}\,\tau^{-1/2}$, limited by a flicker floor of 1.5×10^{-16} between 100 s and 5,000 s.

One of these CSOs (Fig. 8), was specifically designed to be transported in a small truck, intended to test the technology and to evaluate its potential for real applications. In a few years ULISS accomplished 9 roundtrips visiting 7 different European locations, the farthest of which is Goteborg, Sweden, and traveled more than 10,000 km [33]. No damage, degradation of stability loss has ever occurred after partial disassembling and reassembling the CSO to fit it in the truck.

The ULISS *Odissey* was the opportunity to meet potential users, with the obvious purpose of understanding their needs and the difficulties related to the installation of a CSO in their lab [34], [35], [36]. This experience revealed that the high electrical power needed by the compressor (380 V three-phase line, 6 kW stationary) is the major problem, together with the amount of heat generated—albeit the latter is mitigated by the fact that the compressor is generally located outside the controlled metrological area. Such problems hinder the deployment of the CSO technology.

IV. ULISS-2G: 2ND GENERATION OF CRYCOOLED CSOS

The ULISS-2G project was launched to solve the high electrical power required by the 1st generation CSOs. The cryostat was redesigned and optimized for the new spec of 3 kW, single-phase, matching the available power from a regular 230 V, 16 A outlet. This means capability to maintain a temperature down to ~ 4 K with the cooling power of 250 mW of the Cryomech PT403 Pulse-Tube [37]. This was achieved by improving the thermal shielding, the conductance and the flexibility of copper braids, and by designing new 3D-printed Mylar holding rods. Designing a new cryostat was also an opportunity to shrink the size and to rationalize the assembly: the supporting frame was suppressed and replaced with the vacuum can itself, now more rigid [20]. This allowed to place the cryostat in a 19" rack, together with the control electronics and the frequency synthesizer. Fig. 9 shows ULISS-2G with its water-cooled compressor.

Since 2017, we build and validated six ULISS-2G CSOs of identical design. The only notable difference between them is the value of the resonator turnover temperature T_0. Fig. 10 shows the Allan deviation of these CSOs, obtained comparing the CSO under test to two 1st-generation CSOs of Oscillator IMP, with the three-cornered-hat configuration. The Allan deviation of all the ULISS-2G CSOs is better than 3×10^{-15} for $1\,\mathrm{s} \le \tau \le 10{,}000\,\mathrm{s}$, with a drift below 1×10^{-14} per day.

At short term, $1\,\mathrm{s} \le \tau \le 100\,\mathrm{s}$, none of the CSOs is limited by the noise of the Pound frequency discriminator, which is always below $7\times10^{-15}\tau^{-1/2}$. Here, the CSO frequency stability is limited by the residual temperature fluctuations affecting the resonator. In [28], we have shown how unexpected time lag in the thermal system and the relative slowness of the digital temperature control induce small and slow temperature

Figure 9. ULISS-2G, the 2nd generation CSO. Notice the He compressor significantly smaller than that of Fig. 8, which takes 3 kW and can be powered from a common 230 V, 16 A outlet.

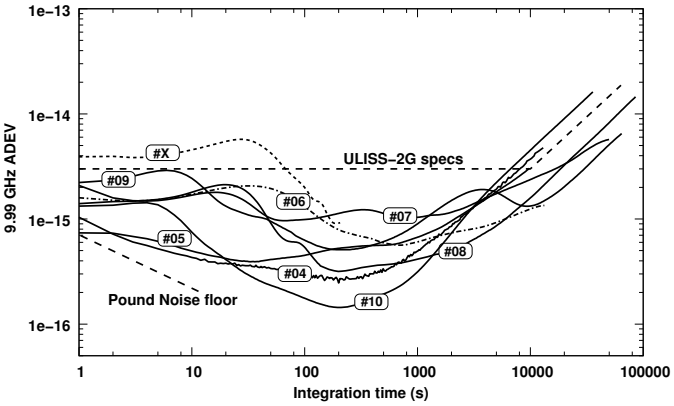

Figure 10. Fractional frequency stability of the ULISS-2G CSOs, drift not removed. CSO #04 is the first prototype described in [20]. CSO #X uses a non-compliant resonator with $T_0 \sim 9$ K, which has been discarded. See Table I for the identification of the CSOs.

modulation in the resonator. This modulation originates bumps in the ADEV curve of five CSOs, clearly visible in Fig. 7 between 5 s and 100 s. Our confidence in this interpretation is supported by the fact that the best two ULISS-2G CSOs, #04 and #05, are characterized by a resonator turnover temperature of 5.1 K and 5.2 K, the turnover of units #6–#10 occurs between 6.9 K and 7.3 K.

Curve #X was obtained with a non-compliant resonator characterized by $T_0 = 9.0$ K. Despite the high Q, $\sim 10^9$, the short-term ADEV is higher than the ULISS-2G spec $\sigma_y(\tau) \leq 3{\times}10^{-15}$. This resonator was discarded.

The CSO #10, the last implemented, has been started in March 2022, and it is still being tested at FEMTO-ST, catching attention because of the very good medium-term stability, close to $1{\times}10^{-16}$ around 200 s. The turnover temperature is of 6.2 K.

The differences between the nearly identical CSOs can be explained by considering the temperature sensitivity of the following parameters.

1) Residual thermal sensitivity of the resonator: near T_0, the resonator frequency is well approximated by the quadratic law $\nu(T) = \nu(T_0)\left[1 + a(T - T_0)^2\right]$, where $a < 0$ is the curvature, in K^{-2}. Thus, the thermal sensitivity close to the turning point is

$$\frac{1}{\nu_0}\frac{\Delta\nu}{\Delta T} = 2a(T - T_0) \tag{1}$$

The curvature a depends on T_0, and in the considered temperature range $a \propto T_0^2$. Thus, a increases by a factor of two from 5 K to 7 K.

2) Sensibility of the temperature sensor: the cryogenic sensors we use are zirconium-nitride thin-film resistors. Their typical sensitivity, in Ω/K, decreases by a factor of 1/5 from 5 K to 7 K [38].

3) Physical properties of materials: the thermal conductivity k, in $\mathrm{W\,m^{-1}\,K^{-1}}$, and the heat capacity C_p, in $\mathrm{J\,kg^{-1}\,K^{-1}}$, of virtually all materials increase significantly from 5 K to 7 K [39]. For Copper, $k \propto T$ has relatively little importance, but C_p doubles from 5 K to 7 K. For sapphire, k and C_p are both proportional to T^3.

All the above described phenomena indicate that the lowest turning point is advantageous in that the temperature control is more efficient: lower temperature sensitivity of the resonator, smaller thermal time constants, and higher sensitivity of the temperature sensor.

A long term, $\tau > 100$ s, the frequency stability is mainly limited by the ambient temperature variations. For slow variations, the estimated sensitivity is $1{\times}10^{-14}\ \mathrm{K}^{-1}$. All CSOs of Fig. 10 were tested in a workshop with usual on-off air-conditioning. Depending on the sunlight, the temperature near the cryostat varies of several degrees during the day. Moreover, the workshop is on free access for the laboratory staff, which makes impossible to keep the environment unperturbed for the duration of the measurement (few days).

V. Maintenance, Mechanical Robustness and Failure Report

The electronics needs no maintenance, and we never experienced a failure in the Pound control or in the power control. That said, metrology at this level of stability obviously requires continuous monitoring. The refrigerator requires replacing every 2nd year a Helium filter at the input of the compressor. The operation is easily done by the user. It requires 1/2 hour manpower, but the compressor is stopped for 1 hour. At the end the cryostat is still cold enough for the CSO to be operational at full stability after half a day.

The experience with ELISA, delivered to Malargüe, and with the 9 roundtrips of ULISS are per se a proof of mechanical robustness. We experienced only two failures since the beginning of the experience reported, the rotary valve of a PT, and a tunnel diode. In both cases the CSO recovered at full stability.

The rotary valve caused the refrigerator not to restart after a scheduled stop. It could have failed at a different time stopping

the machine, but fortunately it did not. Having the spare part on the shelf, the replacement took 1/2 hour working time. Anomalous mechanical wear is the most accredited reason.

A tunnel diode in the power control had to be replaced after showing a progressive degradation of sensitivity. This let us time to schedule a stop without sudden signal loss, but the replacement required to disassemble the cryostat, and to restart vacuum and cooling. Thermal stress is the most accredited reason, given the fact that this type of diode is not specified for cryogenic environment by the manufacturer, but it was qualified in our lab after appropriate tests. The diode, installed in a machine intended for R&D tests whose cryostat has been disassembled numerous times, has undergone an excess of thermal cycles. For this reason, we do not consider such failure a risk under normal circumstances.

VI. Summary

We reported on our experience building a dozen of cryogenic sapphire oscillators (CSOs) since 2009.

Describing the stability as Allan deviation $\sigma_y(\tau)$ of the fractional frequency y as a function of the measurement time τ, the CSO outperforms all other technologies in the region defined by $1\text{s} < \tau < 10^4$ s, where $\sigma_y(\tau) < 3{\times}10^{-15}$ (specs), down to parts in 10^{-16} in the central part. The maximum drift is $1{\times}10^{-14}$ over one day. Some of the CSOs have been running continuously for years with no noticeable aging.

All CSOs proved to be reliable in the long term, and resistant to intercontinental travels. In this long experience we had only two failures, in development prototypes that have been disassembled and reassembled multiple times.

The new design, which reduces the need of electrical power from 6–8 kW three-phase to 3 kW single-phase, is now a semicommercial product available to qualified users.

References

[1] S. Stein and J. Turneaure, "Superconducting-cavity-stabilised oscillator of high stability," *Electronics Letters*, vol. 13, no. 8, pp. 321–323, 1972.

[2] S. Stein, "Space applications of superconductivity: resonators for high stability oscillators and other applications," *Cryogenics*, vol. 20, no. 7, pp. 363–371, 1980.

[3] D. Strayer, G. Dick, and E. Tward, "Superconductor-sapphire cavity for an all-cryogenic SCSO," *IEEE Transactions on Magnetics*, vol. 19, no. 3, pp. 512–515, 1983.

[4] D. Blair and S. Jones, "High-Q sapphire loaded superconducting cavities and application to ultrastable clocks," *IEEE Transactions on Magnetics*, vol. 21, no. 2, pp. 142–145, 1985.

[5] C. D. Langham and J. C. Gallop, "Development of a high stability cryogenic sapphire dielectric resonator," *IEEE Transactions on Instrumentation and Measurement*, vol. 42, no. 2, pp. 96–98, 1993.

[6] O. Di Monaco, W. Daniau, I. Lajoie, Y. Gruson, M. Chaubet, and V. Giordano, "Modal selection for a whispering gallery mode resonator," *Electronics Letters*, vol. 32, pp. 669–670, Mar. 28, 1996.

[7] A. N. Luiten, A. G. Mann, and D. G. Blair, "Cryogenic sapphire microwave resonator oscillator with exceptional stability," *Electronics Letters*, vol. 30, pp. 417–418, Mar. 3 1994.

[8] R. T. Wang and G. J. Dick, "Cryocooled sapphire oscillator with ultra-high stability," *IEEE Transactions on Instrumentation and Measurement*, vol. 48, pp. 528–531, Apr. 1999.

[9] G. Santarelli, P. Laurent, P. Lemonde, A. Clairon, A. G. Mann, S. Chang, A. N. Luiten, and C. Salomon, "Quantum projection noise in an atomic fountain: A high stability cesium frequency standard," *Physical Review Letters*, vol. 82, June 1999.

[10] S. Chang, A. G. Mann, and A. N. Luiten, "Improved cryogenic sapphire oscillator with exceptionally high frequency stability," *Electronics Letters*, vol. 36, pp. 480–481, Mar. 2 2000.

[11] P. Wolf, S. Bize, A. Clairon, A. N. Luiten, G. Santarelli, and M. E. Tobar, "Test of Lorentz invariance using a microwave resonator," *Physical Review Letters*, vol. 90, pp. 060402–1–4, Feb. 14 2003.

[12] P. Y. Bourgeois, F. Ladret-Vieudrin, Y. Kersalé, N. Bazin, M. Chaubet, and V. Giordano, "Ultra low drift microwave cryogenic oscillator," *Electronics Letters*, vol. 40, May 13 2004.

[13] P. Y. Bourgeois, Y. Kersalé, N. Bazin, M. Chaubet, and V. Giordano., "A cryogenic open-cavity sapphire reference oscillator with low spurious mode density.," *IEEE Transactions on Ultrasonics, Ferroelectrics and Frequency Control*, vol. 51, Oct. 2004.

[14] G. J. Dick and N. Wang, "Stability and phase noise tests of two cryo-cooled sapphire oscillators," *IEEE Transactions onUltrasonics, Ferroelectrics, and Frequency Control*, vol. 47, no. 5, pp. 1098–1101, 2000.

[15] S. Grop, P. Y. Bourgeois, N. Bazin, Y. Kersalé, E. Rubiola, C. Langham, M. Oxborrow, D. Clapton, S. Walker, J. De Vicente, and V. Giordano, "ELISA: A cryocooled 10 GHz oscillator with 10^{-15} frequency stability," *Review of Scientific Instruments*, vol. 81, no. 2, p. 025102, 2010.

[16] https://quantxlabs.com/.

[17] V. Giordano, S. Grop, P.-Y. Bourgeois, Y. Kersalé, and E. Rubiola, "Influence of the electron spin resonance saturation on the power sensitivity of cryogenic sapphire resonators," *Journal of Applied Physics*, vol. 116, no. 5, pp. 054901(1–7), 2014.

[18] V. Giordano, C. Fluhr, and B. Dubois, "Magnetic sensitivity of the microwave cryogenic sapphire oscillator," *Journal of Applied Physics*, vol. 127, no. 18, p. 184101, 2020.

[19] S. Grop, W. Schäfer, P.-Y. Bourgeois, Y. Kersalé, M. Oxborrow, E. Rubiola, and V. Giordano, "Unprecedented high long term frequency stability with a microwave resonator oscillator," *IEEE Transactions on Ultrasonics, Ferroelectrics and Frequency Control*, vol. 58, May 24, 2011.

[20] C. Fluhr, B. Dubois, S. Grop, J. Paris, G. Le Tetû, and V. Giordano, "A low power cryocooled autonomous ultra-stable oscillator," *Cryogenics*, vol. 80, pp. 164–173, 2016.

[21] T. Kessler, C. Hagemann, C. Grebing, T. Legero, U. Sterr, F. Riehle, M. Martin, L. Chen, and J. Ye, "A sub-40-mHz-linewidth laser based on a silicon single-crystal optical cavity," *Nature Photonics*, vol. 6, no. 10, pp. 687–692, 2012.

[22] J. M. Robinson, E. Oelker, W. R. Milner, W. Zhang, T. Legero, D. G. Matei, F. Riehle, U. Sterr, and J. Ye, "Crystalline optical cavity at 4 K with thermal-noise-limited instability and ultralow drift," *Optica*, vol. 6, no. 2, pp. 240–243, 2019.

[23] https://www.menlosystems.com/products/ultrastable-lasers/ors/.

[24] https://stablelasers.com/.

[25] S. Grop, P. Y. Bourgeois, R. Boudot, Y. Kersalé, E. Rubiola, and V. Giordano, "10 GHz cryocooled sapphire oscillator with extremely low phase noise," *Electronics Letters*, vol. 46, pp. 420–422, 18th March 2010.

[26] S. Grop, P.-Y. Bourgeois, E. Rubiola, W. Schäfer, J. De Vicente, Y. Kersalé, and V. Giordano, "Frequency synthesis chain for the ESA deep space network," *Electronics Letters*, vol. 47, pp. 386–388, Mar. 17, 2011.

[27] V. Giordano, S. Grop, C. Fluhr, B. Dubois, Y. Kersalé, and E. Rubiola, "The autonomous cryocooled sapphire oscillator: A reference for frequency stability and phase noise measurements," *Journal of Physics: Conference Series*, vol. 723, no. 1, p. 012030, 2016.

[28] C. Fluhr, S. Grop, B. Dubois, Y. Kersalé, E. Rubiola, and V. Giordano, "Characterization of the individual short-term frequency stability of cryogenic sapphire oscillators at the 10^{-16} level," *IEEE Transactions on Ultrasonics, Ferroelectrics and Frequency Control*, vol. 63, no. 6, pp. 915–921, 2016.

[29] V. Giordano, C. Fluhr, S. Grop, and B. Dubois, "Tests of sapphire crystals manufactured with different growth processes for ultra-stable microwave oscillators," *IEEE Transactions on Microwave Theory and Techniques*, vol. 64, pp. 78–85, Jan. 2016.

[30] V. Giordano, C. Fluhr, B. Dubois, and E. Rubiola, "Characterization of zero-bias microwave diode power detectors at cryogenic temperature," *Review of Scientific Instruments*, vol. 87, no. 8, p. 084702, 2016.

[31] C. R. Locke, E. N. Ivanov, J. G. Hartnett, P. L. Stanwix, and M. E. Tobar, "Invited article: Design techniques and noise properties of ultrastable cryogenically cooled sapphire-dielectric resonator oscillators," *Review of Scientific Instruments*, vol. 79, no. 5, 2008.

[32] https://www.femto-engineering.fr/en/equipement/oscillator-instability-measurement-platform/.

[33] V. Giordano, S. Grop, B. Dubois, P.-Y. Bourgeois, Y. Kersalé, E. Rubiola, G. Haye, V. Dolgovskiy, N. Bucalovicy, G. D. Domenico, S. Schilt, J. Chauvin, and D. Valat, "New generation of cryogenic sapphire

microwave oscillator for space, metrology and scientific applications," *Review of Scientific Instruments*, vol. 83, no. 8, 2012.

[34] S. Grop, B. Dubois, J.-L. Masson, G. Haye, P.-Y. Bourgeois, Y. Kersalé, E. Rubiola, and V. Giordano, "Uliss project: First comparison of two cryocooled sapphire oscillators at the 10^{-15} level," in *2012 IEEE International Frequency Control Symposium Proceedings*, pp. 1–5, IEEE, 2012.

[35] V. Dolgovskiy, S. Schilt, N. Bucalovic, G. Di Domenico, S. Grop, B. Dubois, V. Giordano, and T. Südmeyer, "Ultra-stable microwave generation with a diode-pumped solid-state laser in the 1.5-μm range," *Applied Physics B*, vol. 116, no. 3, pp. 593–601, 2014.

[36] M. Abgrall, J. Guéna, M. Lours, G. Santarelli, M. Tobar, S. Bize, S. Grop, B. Dubois, C. Fluhr, and V. Giordano, "High-stability comparison of atomic fountains using two different cryogenic oscillators," *IEEE Transactions on Ultrasonics, Ferroelectrics, and Frequency Control*, vol. 63, no. 8, pp. 1198–1203, 2016.

[37] http://www.cryomech.com/.

[38] S. S. Courts and P. R. Swinehart, "Review of Cernox™ (Zirconium Oxy-Nitride) thin-film resistance temperature sensors," in *AIP Conference Proceedings*, vol. 684, pp. 393–398, American Institute of Physics, 2003.

[39] S. W. V. Sciver, "Low-temperature materials properties," in *Helium Cryogenics*, pp. 17–58, Springer, 2012.